Nonlinear Coupling of Phononic Resonators Induced by Surface Acoustic Waves

Sarah Benchabane,* Aymen Jallouli, Laetitia Raguin, Olivier Gaiffe, Jules Chatellier, Valérie Soumann, Jean-Marc Cote, Roland Salut, and Abdelkrim Khelif

Franche-Comté Électronique Mécanique Thermique et Optique—Sciences et Technologies (FEMTO-ST), Université de Bourgogne Franche-Comté, CNRS, UFC 15B Avenue des Montboucons, Besançon Cedex F-25030, France

(Received 28 July 2021; revised 1 October 2021; accepted 8 October 2021; published 11 November 2021)

The rising need for hybrid physical platforms has triggered a renewed interest in the development of agile radio-frequency phononic circuits with complex functionalities. The combination of traveling waves with resonant mechanical elements appears as an appealing means of harnessing elastic vibration. In this work, we demonstrate that this combination can be further enriched by the occurrence of traveling surface acoustic waves (SAWs), induced by elastic nonlinearities, interacting with a pair of otherwise linear micron-scale mechanical resonators. Reduction of the resonator-gap distance and an increase in the SAW amplitude results in a frequency softening of the resonator-pair response that lies outside the usual picture of geometrical Duffing nonlinearities. The dynamics of the SAW excitation scheme allows further control of the resonator motion, notably leading to circular-polarization states. These results may pave the way toward versatile high-frequency phononic microelectromechanical-systems–nanoelectromechanical-systems circuits fitting both classical and quantum technologies.

DOI: 10.1103/PhysRevApplied.16.054024

I. INTRODUCTION

The on-chip manipulation of elastic or mechanical vibrations, whether hosted and localized within resonators or traveling in the material substrate, has been leading to significant progress in diverse areas of applied and fundamental science. Surface-acoustic-wave (SAW) devices are a striking example of such rapid developments. They are ubiquitously used in modern telecommunications systems [1] and are extremely relevant as sensing components in a number of applications [2,3]. Micro- and nanomechanical systems, for their part, have imposed themselves as prevalent means of implementing extremely sensitive sensing devices [4–6]. They are characterized by a rich dynamics, involving linear and nonlinear phenomena [7–10] that opens exciting prospects for mechanical signal processing. This dynamics can be further enriched in coupled systems where mechanical mode coupling can be induced in, e.g., clamped beams [11–13], pillars [14,15], or through intermodal coupling [16–19]. Over the past few years, both types of mechanical systems have been attracting renewed interest [20] and have been exploited to achieve dynamic and coherent interaction with a variety of physical systems, including holes and electrons [21–23], quantum dots [24–27], spins [28,29], superconducting circuits [30–33], and photonic devices [34–37]. The enhancement of control over such mechanical systems at the micro- or nanoscale and in the radio-frequency (rf) regime therefore holds promise for the implementation of complex phononics-based hybrid platforms permitting high-speed operation. A number of works have proposed to combine mechanically resonant elements with traveling elastic waves to demonstrate dynamic linear and nonlinear phononic systems, whether in the context of phononic crystals and elastic metamaterials [38–43] or in nanoelectromechanical-systems- (NEMS) based architectures [44,45]. In the last case, the reported devices exploit geometric, electrostatic, or wave-mixing-induced nonlinear behaviors, taking advantage of the high-quality-factor resonance of mechanical elements. The current limit of this approach, however, lies in the attainable resonant frequencies, which are heavily conditioned by NEMS classically operating at maximum frequencies of a few megahertz.

In this work, we demonstrate the possibility of implementing a nonlinear phononic platform based on the interaction of traveling SAWs and coupled mechanical resonators capable of operating in the rf regime. We analyze a pair of low-aspect-ratio cylindrical pillars vibrating on a flexural mode and demonstrate the unexpected nonlinear coupled mechanical states obtained from these otherwise linearly behaving mechanical resonators. The observed experimental results, supported by analytical modeling and numerical simulations, show that these nonlinearities are the result of an interplay between the resonator-mode

*sarah.benchabane@femto-st.fr

symmetry and the elastic field distribution on the substrate surface and that they exhibit a strong dependence on the resonator-gap distance and the SAW excitation scheme. In turn, the elastic energy distribution affects the substrate surface displacement, hence disturbing the resonator dynamics and leading to the occurrence of a circular state of motion. The proposed devices, which operate in the 70-MHz range, are readily scalable to higher frequencies. They illustrate the relevance of SAW-based phononic devices for the implementation of high-frequency electromechanical circuits with complex dynamics.

II. LINEAR REGIME: SINGLE RESONATORS AND LARGE GAP DISTANCES

The phononic resonators under study consist of micron-scale cylindrical pillars with an aspect ratio of the order of one, deposited atop a single-crystal piezoelectric substrate. The resonators are excited by a Rayleigh-surface acoustic wave generated by an interdigital transducer (IDT) harmonically driven at frequencies of about 70 MHz. The resulting SAW amplitude depends linearly on the applied rf power. The mode of interest is a first-order flexural mode, which is theoretically composed of two degenerate orthogonally polarized eigenstates due to the circular cross section of the resonators. The frequency response of isolated SAW-coupled resonators has previously been shown to exhibit Fano line shapes, resulting from the interaction of the impinging SAW with the localized mechanical resonator [14]. Figure 1(a) reports the out-of-plane vibration amplitude measured out of a single resonator subjected to a SAW driven by rf input powers ranging from 10 to 20 dBm. A single resonance peak appears at a frequency of 70.7 MHz. The degeneracy lifting expected from fabrication imperfections in resonators with circular symmetries cannot be observed here. This can be accounted for by the low quality factor (Q factor) of the resonance, which is equal to about 30. When increasing the drive power, the vibration amplitude of the phononic resonator shows a predictable linear dependency, as expected from such low-Q-factor mechanical structures under the present weak excitation, with a constant resonant frequency and Q factor.

Similar experiments have been conducted on a pillar pair with a 6-μm gap distance excited by a SAW with a wave vector directed along the inter-resonator axis. Figure 1(b) shows that increasing the SAW drive power again leaves the frequency position and Q factor of the pillar-pair resonances unaffected. Here, therefore, the coupling mechanism is independent of the SAW amplitude, as expected for linearly strain-coupled mechanical resonators.

III. FREQUENCY SOFTENING IN SMALLER-GAP-DISTANCE COUPLED-RESONATOR SYSTEMS

The previous observations do not hold, however, for shorter gap distances, where SAW-mediated dipolelike

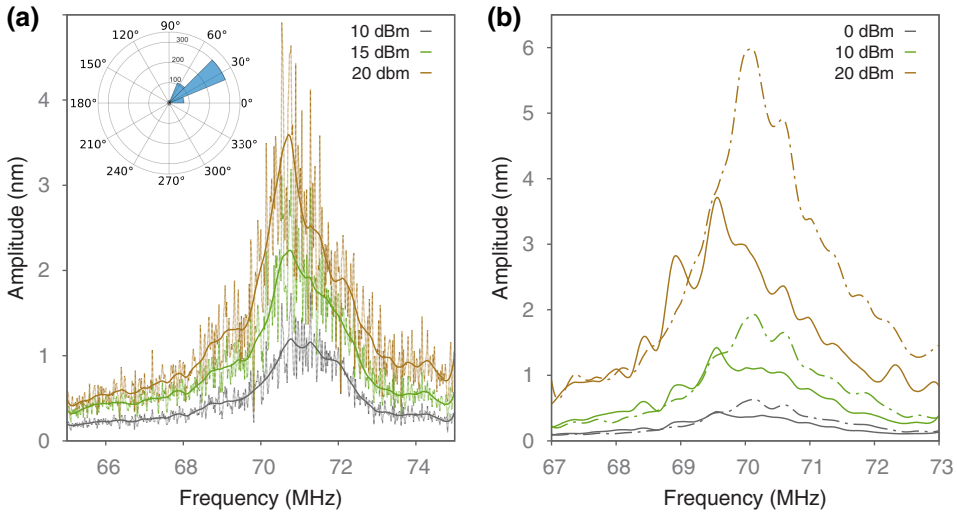

FIG. 1. The experimental frequency responses of SAW-driven phononic microresonators. (a) The response of a single pillar with a diameter of 4.4 μm and a height of about 4 μm excited by a SAW for different input powers applied to the IDT (10 dBm, 15 dBm, and 20 dBm). The light dotted lines correspond to data obtained by laser-scanning interferometry and acquired every 10 kHz. The solid lines are obtained by applying a Savitsky-Golay smoothing filter to the raw experimental data. The inset shows an angular plot of the distribution of the orientation of the flexural-mode vibration for frequencies between 65 and 75 MHz. (b) The frequency response for two pillars within a pair with a 6-μm gap distance excited by a longitudinal SAW wave vector under different drive powers. The solid line corresponds to the resonator located closest to the SAW source and the dashed line to the resonator located farthest from the source.

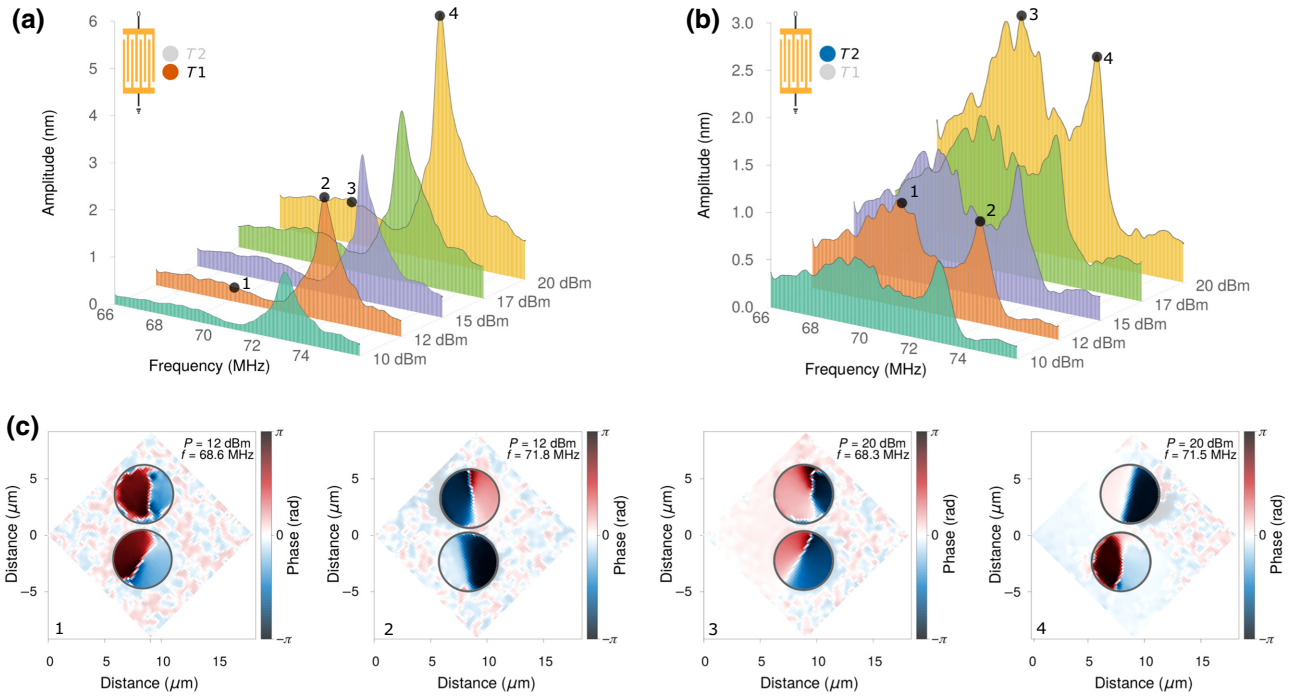

FIG. 2. The experimental frequency and phase responses of a pillar pair excited by a transverse SAW. The gap distance is 1.5 μm. (a) The response of resonator $T1$. (b) The response of resonator $T2$. (c) Experimental phase maps at 12 dBm for the lower-frequency mode (i) at 68.6 MHz (1) and for the higher-frequency mode (ii) at 71.8 MHz (2); and at 20 dBm for the lower-frequency mode (i) at 68.3 MHz (3) and for the higher-frequency mode (ii) at 71.5 MHz (4).

interaction is dominant [14]. A similar investigation of the resonator response as a function of the drive power is performed for 1.5-μm-spaced pillar pairs excited by SAWs propagating either along the inter-resonator axis (longitudinal excitation) or in the direction normal to the inter-resonator axis (transverse excitation). The results obtained in the case of a transverse excitation are reported in Figs. 2(a) and 2(b) for each resonator, here denoted $T1$ and $T2$. The resonator-pair frequency response reveals the existence of two vibrational modes. The first mode (i) is found at about 68 MHz and has a Q factor of about 30, which is comparable with the one observed for a single pillar. A higher-frequency mode (ii) lying slightly below 72 MHz can also be found, with a Q factor now reaching about 60. The resonance line shape exhibits the lightly asymmetric profile expected in coupled-resonator systems. Increasing the drive power in the 10–20 dBm range results in a down shift of about 400 kHz for mode (ii), while the lower-frequency mode (i) remains at the same frequency position. Phase maps obtained by laser-scanning interferometry and reported in Fig. 2(c) reveal that mode (i) corresponds to a symmetric mode, while mode (ii) corresponds to an antisymmetric mode with respect to the propagation axis. Increasing the drive power in the 10–20 dBm range does not significantly affect the overall modal behavior of the coupled-resonator system.

The observed power-dependent frequency shift hints at a nonlinear coupling of the first-order flexural modes of the two phononic resonators, despite each individual resonator exhibiting an otherwise linear response. The involved nonlinear coupling mechanism is therefore different from those usually exploited in NEMS, which rely on the coupling of high-Q-factor mechanical resonators with geometrical nonlinearities [46,47]. The higher Q factor obtained by resonator-to-resonator coupling could help to trigger nonlinear interactions by lowering the amplitude threshold required to reach the critical point. However, here, these interactions result in a frequency down shift with increasing drive amplitude, while geometrical nonlinearities are expected to result in a frequency up shift in such clamped-free resonators. Such coupling-induced softening nonlinearities have previously been reported in phononic crystals made of local resonators coupled by nonlinear graphene membranes [38]. In our case, coupling occurs through the substrate surface and is mediated by the SAW elastic energy distribution, which is itself conditioned by the resonator-to-resonator coupling conditions. The observed nonlinear behavior can be described as resulting from a softening of the coupling spring constant induced by the highly confined SAW. This effect may allegedly be understood by considering the coupled pillars as forming a cavity for SAW with a strong energy

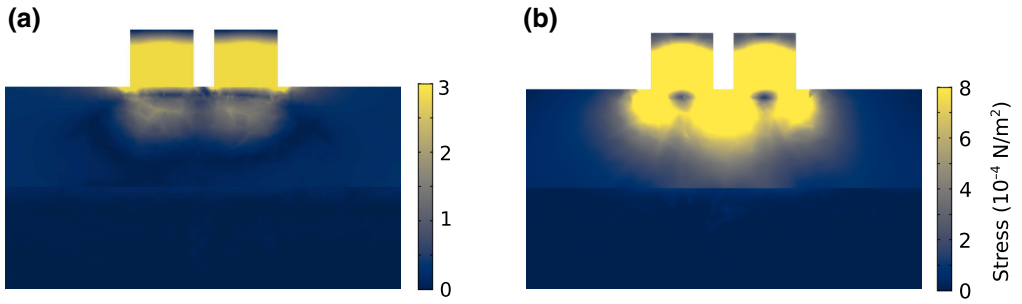

FIG. 3. Finite-element method simulations of the von Mises stress distribution. The two 1.5-μm-spaced resonators are excited by a linear elastic line source following a transverse excitation scheme. (a) Symmetric mode (i), here found at 70.73 MHz. (b) Antisymmetric mode (ii) at 73.34 MHz.

confinement in the 1.5-μm-wide gap. The system becomes resonant, hence promoting energy transfer between the two resonators as the SAW amplitude increases. Finite-element method (FEM) simulations based on a linear elastic model confirm that the phononic resonators induce a strong localization of the elastic energy distribution at the resonator vicinity. The von Mises stress distributions reported in Fig. 3 further highlight that stress localization within the resonator gap is only observed for the antisymmetric mode (ii). This observation is in good agreement with the experimental device response, as only mode (ii) experiences a nonlinear frequency down shift.

As a possible description of this SAW–coupled-resonator system, we propose to use a tentative simplified model based on two single-mode linear oscillators with respective masses m_i $(i = 1, 2)$ coupled by a nonlinear coupling strength k_{nl}. The corresponding equation of motion can be written as

$$m_1\ddot{x_1} + \gamma\dot{x_1} + kx_1 + \kappa_{12}(x_1 - x_2) + \kappa_{\mathrm{nl}}(x_1 - x_2)^3 = F_0\cos(\Omega t), \tag{1a}$$

$$m_2\ddot{x_2} + \gamma\dot{x_2} + kx_2 + \kappa_{12}(x_2 - x_1) + \kappa_{\mathrm{nl}}(x_2 - x_1)^3 = 0, \tag{1b}$$

where x_1 and x_2 are the displacement amplitudes for each resonator, γ is the linear damping, k is the resonator spring constant, and κ_{12} is the linear coupling constant. The unperturbed frequencies of the resonators are defined as $\omega_0^{(i)} = \sqrt{k/m_i}$. The two effective masses are defined from the physical mass of the resonators ($m_i = \rho V_i$, where ρ is the mass density and V_i the volume of the resonators). A difference in mass of about 5%, corresponding to an estimated difference in height of 200 nm between the two resonators, is introduced in the model. The frequency-softening effect is introduced by assuming a negative κ_{nl} constant. The term on the right-hand side corresponds to the SAW excitation, modeled as an external periodic force of strength F_0 and frequency Ω. This external force is applied to only one of the resonators to avoid artificially forcing a relative phase condition between the two oscillators. Figure 4(a) displays the experimental response of the two resonators for a drive power of 20 dBm, along with the corresponding simulated vibration amplitude. The spring constant $k = 116$ (kN/m) and the linear coupling constant $\kappa_{12} = 5.3$ (kN/m) used in the model are estimated from the two resonance frequencies measured for modes (i) and (ii) of the pillar pair (see the Supplemental Material [48]). In order to estimate κ_{nl}, we rewrite the system of Eqs. (1a)–(1b) assuming equal resonator masses ($m_1 = m_2 = m$) (see the Supplemental Material [48]):

$$\ddot{u} + \mu\dot{u} + \omega_0^2 u + \alpha u^3 = F\cos(\Omega t), \tag{2}$$

where $\omega_0 = \sqrt{\frac{k+2\kappa_{12}}{m}}$, $\mu = \gamma/m$, and $\alpha = 2\kappa_{\mathrm{nl}}/m$. $u = x_1 - x_2$ is the amplitude difference between the two resonators. The natural frequency response curve of the nonlinear system can then be described by expressing its backbone curve, which follows a typical parabola shape as a function of the maximum amplitude of u:

$$\Omega = \omega_0 + \frac{3}{8}\frac{\alpha}{\omega_0}a^2, \tag{3}$$

where a represents the amplitude of u. Fitting the experimental resonance frequency at different drive powers to this backbone curve equation, as presented in Fig. 4(b), yields a nonlinear coupling constant κ_{nl} of the order of -0.016 (kN/m^3). The nonlinear coupling term $\pm\kappa_{\mathrm{nl}}(x_1 - x_2)^3$ in Eq. (2) affecting only the out-of-phase mode: the proposed model captures the mode-symmetry dependence of the observed nonlinear effect, with a symmetrical in-phase mode frequency position remaining independent of the drive SAW amplitude.

The occurrence of nonlinearities is confirmed by investigating a similar pillar pair subjected to a longitudinal excitation. The measured frequency responses, reported in Fig. 5, show that the resonator pair, composed by two pillars $L1$ and $L2$, again hosts two sets of modes appearing at the respective frequencies of 71.5 MHz [mode (iii)]

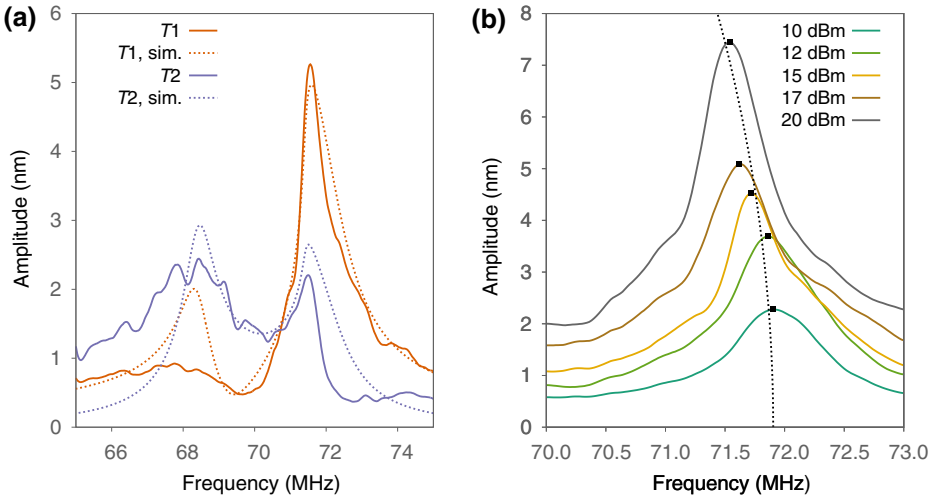

FIG. 4. The coupled-oscillator model of a pillar pair excited by a transverse SAW. (a) The solid lines correspond to the experimental data for a pillar pair with a 1.5-μm gap distance, excited using a rf input power of 20 dBm. The dashed lines correspond to the theoretical frequency response obtained from the proposed coupled-oscillator model for an applied force amplitude $F_0 = 10$ μN. (b) The sum of the measured amplitudes of the two resonators for the antisymmetric mode. The dots indicate the maximum displacement for each input rf power level, while the dashed line is a fit to the theoretical backbone curve given in Eq. (3).

and 73 MHz [mode (iv)] at 10 dBm. An increase in the applied drive power now leads to a frequency down shift for both resonances. The higher-frequency resonance shift is comparable to the one observed in the transverse case and is estimated to be slightly lower than 400 kHz. The resonance frequency of mode (iii) is also down shifted, now with a shift of the order of 600 kHz, as displayed in Fig. 6(a). But one of the most interesting features of this

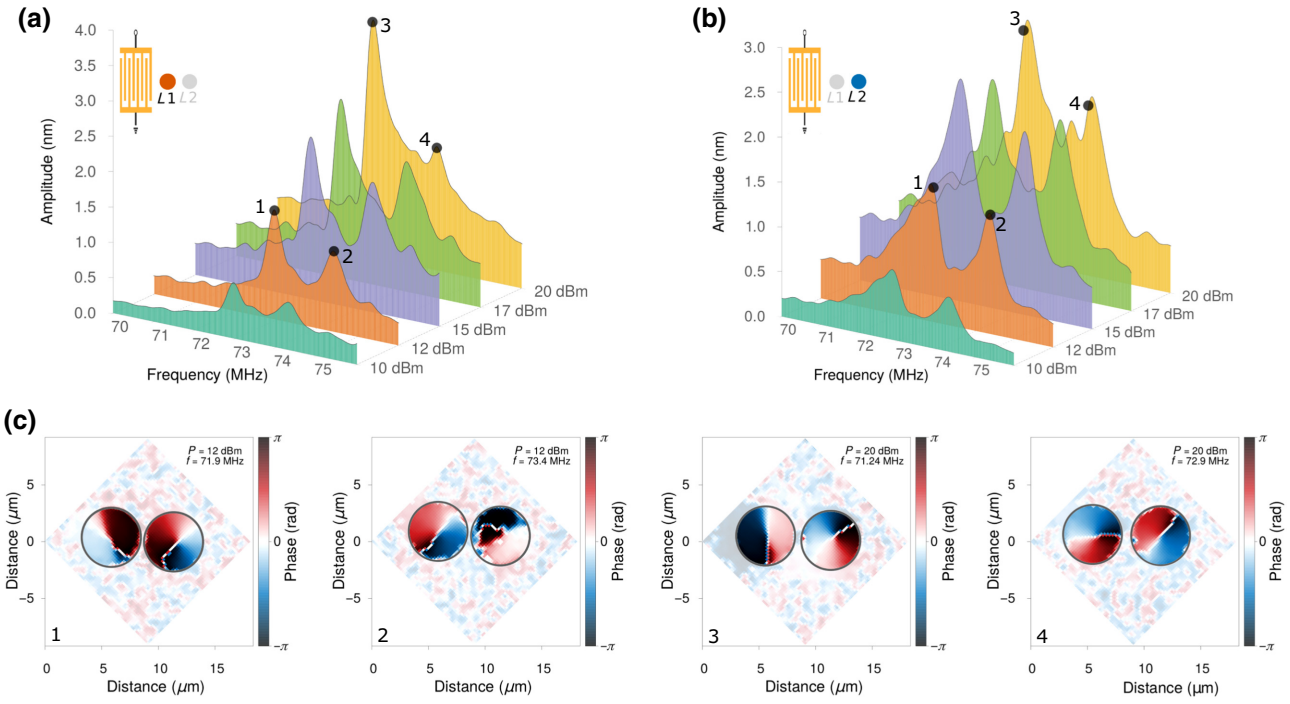

FIG. 5. The experimental frequency and phase responses of a pillar pair excited by a longitudinal SAW. The gap distance is 1.5 μm. (a) The response of resonator *L1*. (b) The response of resonator *L2*. (c) Experimental phase maps at 12 dBm for the lower-frequency mode (iii) at 71.9 MHz (1) and for the higher-frequency mode (iv) at 73.4 MHz (2); and at 20 dBm for the lower-frequency mode (iii) at 71.24 MHz (3) and for the higher-frequency mode (iv) at 72.9 MHz (4).

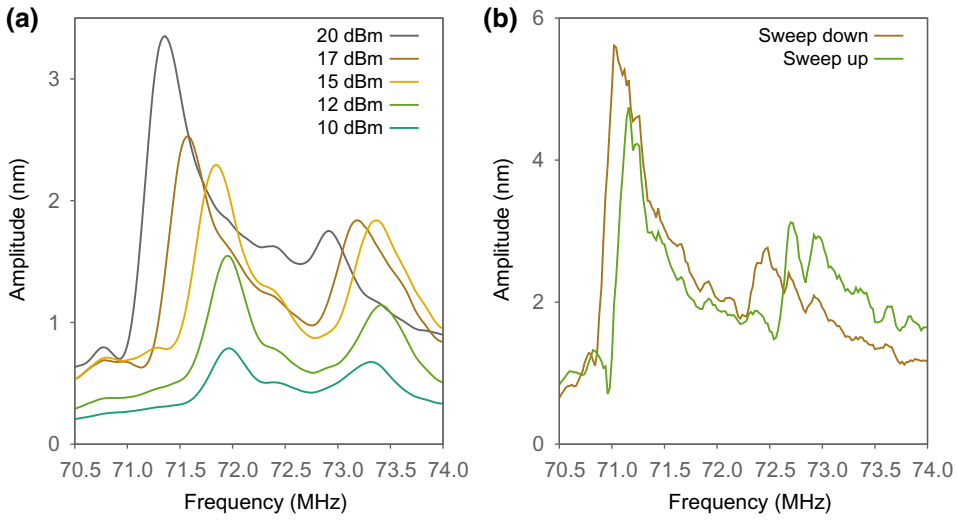

FIG. 6. The hysteresis cycle. (a) The frequency response of resonator $L1$ for varying input powers. (b) A comparison of up and down frequency sweeps for the first resonance of pillar $L1$ (closest to the excitation source) at a rf input power of 20 dBm. The frequency shift linked to the hysteresis cycle appears at about 70.9 MHz.

frequency response lies in the observed change in the resonance profile, which presents an increasing asymmetry as the amplitude increases. This effect leads to a frequency-instability area, which is further confirmed by performing reverse frequency sweeps. Figure 6(b) compares upward and downward frequency sweeps for pillar $L1$, situated closer to the excitation source at 20 dBm. A typical hysteresis cycle is observed, showing an amplitude jump. This behavior confirms the presence of nonlinearities in the proposed system, a rather unexpected result given the geometrical characteristics and operating frequencies of the mechanical resonators involved.

IV. CIRCULARLY POLARIZED RESONANCES

The experimental field maps of Fig. 5(c) further reveal that the input SAW amplitude also affects the nature of the resonator polarization states and breaks the flexural-mode symmetry previously observed in transversely coupled resonators. In the transverse excitation case reported in Fig. 2, only pure flexural modes are observed and the out-of-plane component of the displacement field exhibits a well-defined nodal line, as seen in the phase maps in Fig. 2(c). The corresponding phase states are further depicted in Figs. 7(a) and 7(b), which represent the radial phase of the two resonators extracted from these field maps for an input power of 20 dBm. The two resonators are shown to oscillate either in phase [Fig. 7(a)] or out of phase [Fig. 7(b)], depending on the considered vibration mode. But a longitudinal excitation leads to the occurrence of circular-polarization states. In the case of mode (iii), only one of the two resonators is circularly polarized, while the other one keeps a well-defined flexural behavior [Fig. 7(c)]. The phase state is table over the power range, as shown in the phase maps labeled (1) and (2) in Fig. 5(c), taken at a drive power of 12 dBm. The higher-frequency mode (iv), which appears at a frequency of about 72.9 MHz at 20 dBm, is, however, characterized by circularly polarized states with opposite handedness [Fig. 7(d)]. This behavior points at a cross-coupling between the two orthogonal polarization states that theoretically compose the first-order flexural mode of such resonators with cylindrical symmetry.

The occurrence of these circular states is concomitant with an increase in drive power; they may not, however, indisputably be attributed to nonlinear effects. If nonlinearities have already been shown to induce elliptical polarization states in singly clamped mechanical resonators [46], e.g., in carbon nanotubes [49–51], the elliptical transition is obtained at very high drive powers and can only be obtained from high-Q-factor mechanical resonators. For low Q factors, this elliptical transition is considered trivial and hence independent of any nonlinear behavior. But linear systems can also yield circular-polarization states, provided that the resonators are subjected to force fields with high vorticities [52]. In the present case, the nature of the Rayleigh SAW involves a linearly polarized excitation in the substrate plane. The vibration of the phononic resonator may, however, result in a mechanical back action on the surface acoustic wave field in the vicinity of the resonator, resulting in coupling of the shear-polarization components of the surface displacements. This, in turn, induces cross-coupling of the two orthogonal polarizations of the resonator, hence giving rise to the observed circular-polarization states. This back-action process is, again, triggered by the higher force field induced by the cavity formed in the resonator-to-resonator gap, therefore leading to a power-dependent mechanism.

V. CONCLUSION

In conclusion, we demonstrate the occurrence of surface-acoustic-wave-induced nonlinearities in pairs of otherwise linear coupled phononic microresonators. These nonlinearities are characterized by a frequency softening of the pillar-pair response for short gap distances, while isolated resonators retain a linear behavior. The characteristic

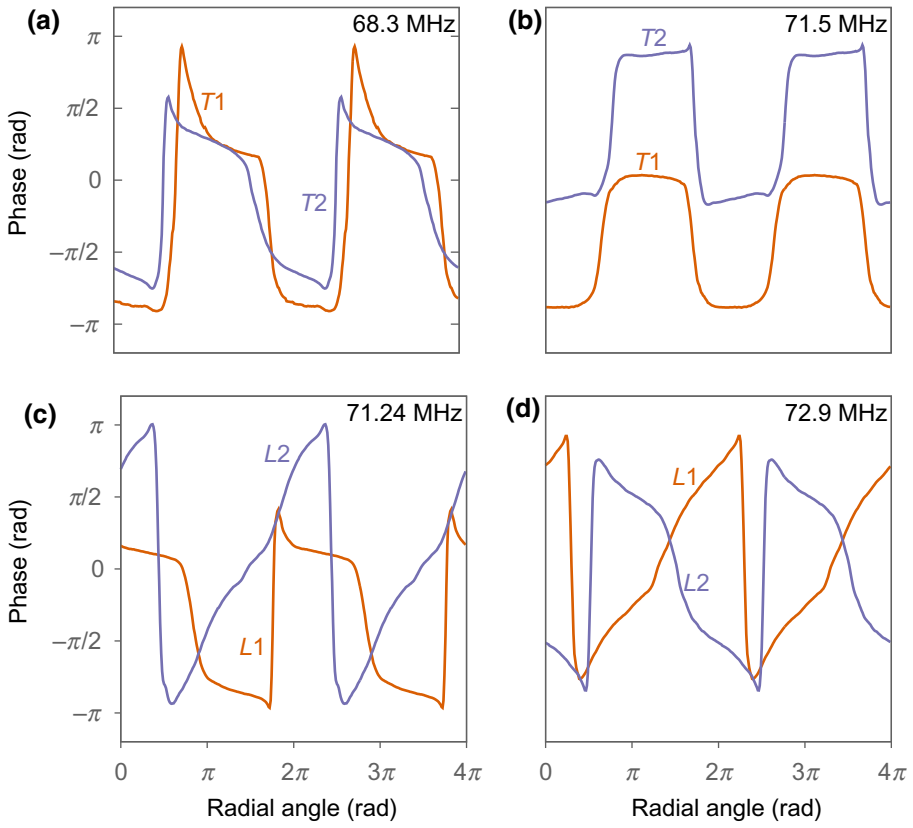

FIG. 7. Typical phase states for the two proposed excitation schemes. The measurements are taken at a drive power of 20 dBm. (a) The symmetric mode at 68.3 MHz and (b) the antisymmetric mode at 71.5 MHz for a transverse excitation. (c) An illustration of rotating polarization states obtained for one of the two resonators in the case of a longitudinal excitation (f = 71.24 MHz) and (d) for both resonators, with opposite handedness, for an excitation frequency of 72.9 MHz. Movies of the corresponding out-of-plane resonator displacements are provided as Supplemental Movies 1–4 in the Supplemental Material [48].

features of the nonlinear response are also conditioned by the incident SAW wave-vector direction. Coupled resonators submitted to a transverse SAW excitation are well described by assuming a negative cubic Duffing-like term applied to the resonator-to-resonator coupling constant, leading to a linear coupling rate of about 5 kN/m and a nonlinear coupling constant of the order of 10^{-2} kN/m^3. In the case of a longitudinal excitation, in addition to the observed nonlinear dynamics, the increased surface displacements in the vicinity of the resonator result in a feedback mechanism between the mechanical motion of the SAW-coupled phononic resonators and the substrate surface that acts as both a clamping element and a source of mechanical excitation. This interaction leads to a cross-coupling of the resonator eigenmodes and hence to the occurrence of rotating polarization states. These results illustrate the rich dynamics involved in these phononic systems, where linear and nonlinear effects can be combined to achieve coherent control of both the frequency response and modal behavior of high-frequency phononic microresonators.

ACKNOWLEDGMENTS

This project has received funding from the European Research Council (ERC) under the European Union's Horizon 2020 research and innovation programme (Grant Agreement No. 865724). This work has also received support from the Agence Nationale de la Recherche under Grant No. ANR-14-CE26-0003-01-PHOREST and from the French RENATECH network with its FEMTO-ST technological facility. A.J. was supported by the EIPHI Graduate School (Contract "ANR-17-EURE-0002").

[1] D. Morgan and E. G. S. Paige, *Surf. Acoust. Wave Filters* (Academic Press, Oxford, 2007), 2nd ed.
[2] D. B. Go, M. Z. Atashbar, Z. Ramshani, and H.-C. Chang, Surface acoustic wave devices for chemical sensing and microfluidics: A review and perspective, Anal. Methods **9**, 4112 (2017).
[3] J. Devkota, P. R. Ohodnicki, and D. W. Greve, SAW sensors for chemical vapors and gases, Sensors **17**, 801 (2017).
[4] M. Li, H. X. Tang, and M. L. Roukes, Ultra-sensitive NEMS-based cantilevers for sensing, scanned probe and very high-frequency applications, Nat. Nanotechnol. **2**, 114 (2007).
[5] K. Jensen, K. Kim, and A. Zettl, An atomic-resolution nanomechanical mass sensor, Nat. Nanotechnol. **3**, 533 (2008).
[6] J. Chaste, A. Eichler, J. Moser, G. Ceballos, R. Rurali, and A. Bachtold, A nanomechanical mass sensor with yoctogram resolution, Nat. Nanotechnol. **7**, 301 (2012).
[7] A. Eichler, J. Chaste, J. Moser, and A. Bachtold, Parametric amplification and self-oscillation in a nanotube mechanical resonator, Nano Lett. **11**, 2699 (2011).

[8] L. G. Villanueva, R. B. Karabalin, M. H. Matheny, D. Chi, J. E. Sader, and M. L. Roukes, Nonlinearity in nanomechanical cantilevers, Phys. Rev. B **87**, 024304 (2013).

[9] P. A. Truitt, J. B. Hertzberg, E. Altunkaya, and K. C. Schwab, Linear and nonlinear coupling between transverse modes of a nanomechanical resonator, J. Appl. Phys. **114**, 114307 (2013).

[10] I. Mahboob, N. Perrissin, K. Nishiguchi, D. Hatanaka, Y. Okazaki, A. Fujiwara, and H. Yamaguchi, Dispersive and dissipative coupling in a micromechanical resonator embedded with a nanomechanical resonator, Nano Lett. **15**, 2312 (2015).

[11] R. B. Karabalin, M. C. Cross, and M. L. Roukes, Nonlinear dynamics and chaos in two coupled nanomechanical resonators, Phys. Rev. B **79**, 165309 (2009).

[12] H. Okamoto, A. Gourgout, C.-Y. Chang, K. Onomitsu, I. Mahboob, E. Y. Chang, and H. Yamaguchi, Coherent phonon manipulation in coupled mechanical resonators, Nat. Phys. **9**, 480 (2013).

[13] T. Faust, J. Rieger, M. J. Seitner, J. P. Kotthaus, and E. M. Weig, Coherent control of a classical nanomechanical two-level system, Nat. Phys. **9**, 485 (2013).

[14] L. Raguin, O. Gaiffe, R. Salut, J.-M. Cote, V. Soumann, V. Laude, A. Khelif, and S. Benchabane, Dipole states and coherent interaction in surface-acoustic-wave coupled phononic resonators, Nat. Commun. **10**, 4583 (2019).

[15] J. Doster, S. Hoenl, H. Lorenz, P. Paulitschke, and E. M. Weig, Collective dynamics of strain-coupled nanomechanical pillar resonators, Nat. Commun. **10**, 5246 (2019).

[16] H. J. R. Westra, M. Poot, H. S. J. van der Zant, and W. J. Venstra, Nonlinear Modal Interactions in Clamped-Clamped Mechanical Resonators, Phys. Rev. Lett. **105**, 117205 (2010).

[17] I. Mahboob, K. Nishiguchi, A. Fujiwara, and H. Yamaguchi, Phonon Lasing in an Electromechanical Resonator, Phys. Rev. Lett. **110**, 127202 (2013).

[18] J. P. Mathew, R. N. Patel, A. Borah, R. Vijay, and M. M. Deshmukh, Dynamical strong coupling and parametric amplification of mechanical modes of graphene drums, Nat. Nanotechnol. **11**, 747 (2016).

[19] M. H. Matheny, J. Emenheiser, W. Fon, A. Chapman, A. Salova, M. Rohden, J. Li, M. H. de Badyn, M. Pósfai, L. Duenas-Osorio, and et al., Exotic states in a simple network of nanoelectromechanical oscillators, Science **363**, eaav7932 (2019).

[20] P. Delsing, A. N. Cleland, M. J. A. Schuetz, J. Knörzer, G. Giedke, J. I. Cirac, K. Srinivasan, M. Wu, K. C. Balram, and C. Bäuerle, *et al.*, The 2019 surface acoustic waves roadmap, J. Phys. D. Appl. Phys. **52**, 353001 (2019).

[21] R. P. McNeil, M. Kataoka, C. J. Ford, C. H. Barnes, D. Anderson, G. A. Jones, I. Farrer, and D. A. Ritchie, On-demand single-electron transfer between distant quantum dots, Nature **477**, 439 (2011).

[22] S. Hermelin, S. Takada, M. Yamamoto, S. Tarucha, A. D. Wieck, L. Saminadayar, C. Bäuerle, and T. Meunier, Electrons surfing on a sound wave as a platform for quantum optics with flying electrons, Nature **477**, 435 (2011).

[23] T.-K. Hsiao, A. Rubino, Y. Chung, S.-K. Son, H. Hou, J. Pedrós, A. Nasir, G. Éthier-Majcher, M. J. Stanley, R. T. Phillips, and et al., Single-photon emission from single-electron transport in a SAW-driven lateral light-emitting diode, Nat. Commun. **11**, 917 (2020).

[24] O. D. Couto, S. Lazi, F. Iikawa, J. A. Stotz, U. Jahn, R. Hey, and P. V. Santos, Photon anti-bunching in acoustically pumped quantum dots, Nat. Photonics **3**, 645 (2009).

[25] M. Metcalfe, S. M. Carr, A. Muller, G. S. Solomon, and J. Lawall, Resolved Sideband Emission of InAs/GaAs Quantum Dots Strained by Surface Acoustic Waves, Phys. Rev. Lett. **105**, 037401 (2010).

[26] J. Kettler, N. Vaish, L. M. de Lépinay, B. Besga, P. L. de Assis, O. Bourgeois, A. Auffèves, M. Richard, J. Claudon, and J. M. Gérard, *et al.*, Inducing micromechanical motion by optical excitation of a single quantum dot, Nat. Nanotechnol. **16**, 283 (2021).

[27] A. Vogele, M. M. Sonner, B. Mayer, X. Yuan, M. Weiß, E. D. S. Nysten, S. F. Covre da Silva, A. Rastelli, and H. J. Krenner, Quantum dot optomechanics in suspended nanophononic strings, Adv. Quantum Technol. **3**, 1900102 (2020).

[28] E. R. MacQuarrie, T. A. Gosavi, N. R. Jungwirth, S. A. Bhave, and G. D. Fuchs, Mechanical Spin Control of Nitrogen-Vacancy Centers in Diamond, Phys. Rev. Lett. **111**, 227602 (2013).

[29] D. A. Golter, T. Oo, M. Amezcua, I. Lekavicius, K. A. Stewart, and H. Wang, Coupling a Surface Acoustic Wave to an Electron Spin in Diamond via a Dark State, Phys. Rev. X **6**, 041060 (2016).

[30] A. D. O'Connell, M. Hofheinz, M. Ansmann, R. C. Bialczak, M. Lenander, E. Lucero, M. Neeley, D. Sank, H. Wang, M. Weides, and et al., Quantum ground state and single-phonon control of a mechanical resonator, Nature **464**, 697 (2010).

[31] M. V. Gustafsson, T. Aref, A. F. Kockum, M. K. Ekstrom, G. Johansson, and P. Delsing, Propagating phonons coupled to an artificial atom, Science **346**, 207 (2014).

[32] K. J. Satzinger, Y. P. Zhong, H.-S. S. Chang, G. A. Peairs, A. Bienfait, M.-H. H. Chou, A. Y. N. Cleland, C. R. Conner, Dumur, and J. Grebel, *et al.*, Quantum control of surface acoustic-wave phonons, Nature **563**, 661 (2018).

[33] A. Bienfait, K. J. Satzinger, Y. P. Zhong, H.-S. Chang, M.-H. Chou, C. R. Conner, É. Dumur, J. Grebel, G. A. Peairs, and R. G. Povey, *et al.*, Phonon-mediated quantum state transfer and remote qubit entanglement, Science **364**, 368 (2019).

[34] D. A. Fuhrmann, S. M. Thon, H. Kim, D. Bouwmeester, P. M. Petroff, A. Wixforth, and H. J. Krenner, Dynamic modulation of photonic crystal nanocavities using gigahertz acoustic phonons, Nat. Photonics **5**, 605 (2011).

[35] K. C. Balram, M. I. Davanço, J. D. Song, and K. Srinivasan, Coherent coupling between radiofrequency, optical and acoustic waves in piezo-optomechanical circuits, Nat. Photonics **10**, 346 (2016).

[36] R. Riedinger, A. Wallucks, I. Marinković, C. Löschnauer, M. Aspelmeyer, S. Hong, and S. Gröblacher, Remote quantum entanglement between two micromechanical oscillators, Nature **556**, 473 (2018).

[37] M. Kalaee, M. Mirhosseini, P. B. Dieterle, M. Peruzzo, J. M. Fink, and O. Painter, Quantum electromechanics of a hypersonic crystal, Nat. Nanotechnol. **14**, 334 (2019).

[38] D. Midtvedt, A. Isacsson, and A. Croy, Nonlinear phononics using atomically thin membranes, Nat. Commun. **5**, 4838 (2014).

[39] Y. Jin, Y. Pennec, B. Bonello, H. Honarvar, L. Dobrzynski, B. Djafari-Rouhani, and M. I. Hussein, Physics of surface vibrational resonances: Pillared phononic crystals, metamaterials, and metasurfaces, Rep. Prog. Phys. **84**, 086502 (2021).

[40] Z.-N. Li, Y.-Z. Wang, and Y.-S. Wang, Nonreciprocal phenomenon in nonlinear elastic wave metamaterials with continuous properties, Int. J. Solids Struct. **150**, 125 (2018).

[41] M. I. Hussein and R. Khajehtourian, Nonlinear Bloch waves and balance between hardening and softening dispersion, Proc. R. Soc. A **474**, 20180173 (2018).

[42] L. Catalini, Y. Tsaturyan, and A. Schliesser, Soft-Clamped Phononic Dimers for Mechanical Sensing and Transduction, Phys. Rev. Appl. **14**, 014041 (2020).

[43] F. Gao, A. Bermak, S. Benchabane, M. Raschetti, and A. Khelif, Nonlinear effects in locally resonant nanostrip phononic metasurface at GHz frequencies, Appl. Phys. Lett. **118**, 113502 (2021).

[44] J. Cha and C. Daraio, Electrical tuning of elastic wave propagation in nanomechanical lattices at MHz frequencies, Nat. Nanotechnol. **13**, 1016 (2018).

[45] M. Kurosu, D. Hatanaka, and H. Yamaguchi, Mechanical Kerr Nonlinearity of Wave Propagation in an On-Chip Nanoelectromechanical Waveguide, Phys. Rev. Appl. **13**, 014056 (2020).

[46] A. H. Nayfeh and D. T. Mook, *Nonlinear Oscillations* (John Wiley & Sons, Ltd., New York, 1979).

[47] A. H. Nayfeh and B. Balachandran, *Applied Nonlinear Dynamics: Analytical, Computational and Experimental Methods* (John Wiley & Sons, Ltd., New York, 1995).

[48] See the Supplemental Material at http://link.aps.org/supplemental/10.1103/PhysRevApplied.16.054024 for a full description of the nonlinear model and for movies of typical experimental measurements of the out-of-plane displacements of the resonators.

[49] S. Perisanu, T. Barois, A. Ayari, P. Poncharal, M. Choueib, S. T. Purcell, and P. Vincent, Beyond the linear and Duffing regimes in nanomechanics: Circularly polarized mechanical resonances of nanocantilevers, Phys. Rev. B **81**, 165440 (2010).

[50] P. Vincent, A. Descombin, S. Dagher, T. Seoudi, A. Lazarus, O. Thomas, A. Ayari, S. T. Purcell, and S. Perisanu, Nonlinear polarization coupling in freestanding nanowire/nanotube resonators, J. Appl. Phys. **125**, 044302 (2019).

[51] W. G. Conley, A. Raman, C. M. Krousgrill, and S. Mohammadi, Nonlinear and nonplanar dynamics of suspended nanotube and nanowire resonators, Nano Lett. **8**, 1590 (2008).

[52] A. Gloppe, P. Verlot, E. Dupont-Ferrier, A. Siria, P. Poncharal, G. Bachelier, P. Vincent, and O. Arcizet, Bidimensional nano-optomechanics and topological backaction in a non-conservative radiation force field, Nat. Nanotechnol. **9**, 920 (2014).